上海交通大學
SHANGHAI JIAO TONG UNIVERSITY

Physics-Informed Learning for EPG-Based TDDB Assessment

Speaker: Wenjie Zhu

Department of Micro/Nano Electronics,
Shanghai Jiao Tong University

CONTENTS PAGE

1. Research Background

Research Background

The TDDB Phenomenon

Time-Dependent Dielectric Breakdown (TDDB) is a key reliability challenge faced by the semiconductor industry in the Cu/Low-k interconnect process, constituting one of the three primary challenges in this domain.

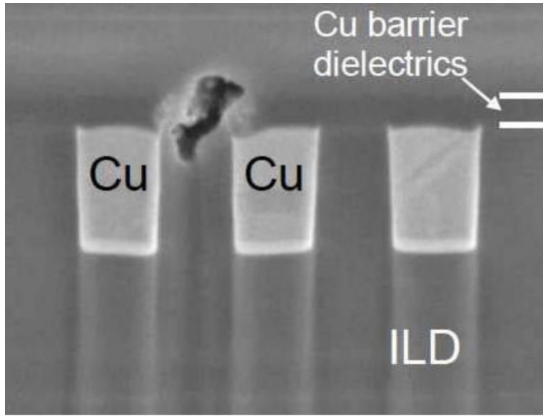

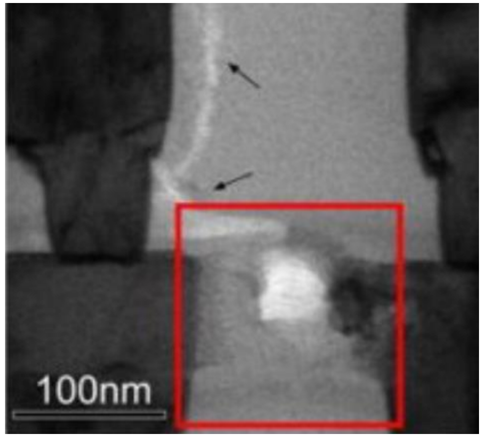

The TDDB phenomenon observed within the inter-layer dielectric (ILD) between two metal layers.

The Cause of TDDB

As the power-on duration of the chip increases, the chip's dielectric is exposed to the electric field for an extended period.

↓

The physical strength of the dielectric gradually weakens under prolonged exposure to the electric field.

↓

When the physical strength of the dielectric weakens to a certain extent, there is a significant probability of dielectric breakdown, resulting in substantial leakage current and causing the chip to fail.

Research Background

☐ TDDB is commonly observed in BEOL (Back End of Line) interconnects.

- **IMD (Inter-Metal Dielectric):**

  IMD refers to dielectric breakdown within the same metal layer caused by electron tunneling current.

- **ILD (Inter-Layer Dielectric):**

  ILD denotes dielectric breakdown between different metal layers.

☐ Time To Failure (TTF)

- TTF refers to the time for a chip to experience **TDDB failure** under a certain level of stress testing. It is crucial for **chip lifespan estimations**, yield calculations, and quality improvement efforts.

Research Objective and Outcome Performance

□ The Primary Objectives

- Constructing a physics-based TDDB model.
- Deriving equations describing TTF from the model.
- Employing physics-informed neural network (PINN) to solve the equations, and comparing the results with the conventional finite element method (FEM).

□ The Performance of the PINN Method

- Compared with the FEM method, the proposed PINN method can lead to about 100 times speedup with less than 0.1% mean squared error.

2. Model and Methodology

Establishment of the TDDB model

- Researchers proposed several TDDB models based on different breakdown mechanisms.

1/E model (I.C.Chen; 1985)

$$\log(TTF) \propto \frac{1}{E_{OX}}$$

E model (J.W.McPherson; 1998)

$$\ln(TTF) \propto \frac{\triangle H_0}{k_B T} - \gamma \cdot E$$

$\sqrt{E}$ model (Scarpulla J)

$$t_{BD} \propto \frac{Q_{BD}}{E} \exp\left(\frac{q\left(\Phi_B - \sqrt{\frac{qE}{\pi \varepsilon_0 \varepsilon_\infty}}\right)}{kT}\right)$$

EPG-based TDDB model (Xin Huang; DAC 2016)

The starting point of our work

The EPG-Based TDDB Model

◻ EPG: Electric Path Generation

The EPG-based TDDB model suggests that the breakdown phenomenon arises from the collective impact of metal ion diffusion and hoping conductivity of the current carriers.

The barrier metal ions (Ta) diffuse into the dielectrics, generating defects which serve as potential centers for localization of electrons.

Electrons leap between adjacent centers, forming a macroscopic resistance network and facilitating current flow.

Breakdown is deemed to take place when the maximum local resistance falls below a threshold (current exceeds the threshold).

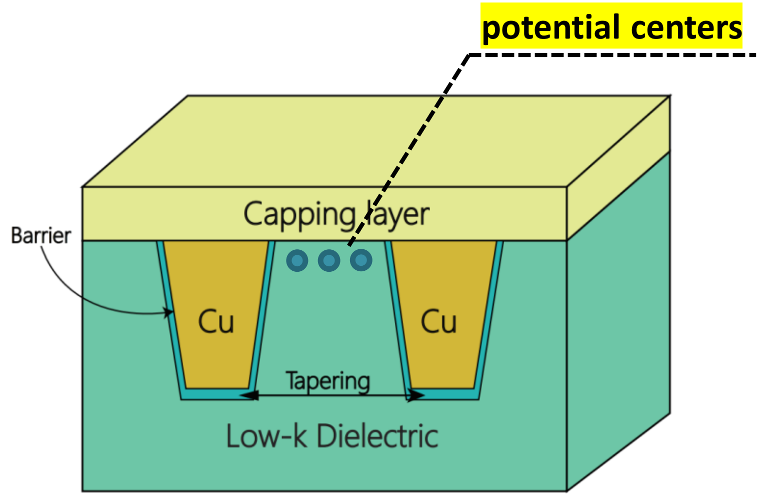

Cross-section of the Cu/low-k structure in IMD

The EPG-Based TDDB Model

☐ The essence of breakdown lies in EPG.

If the maximum local resistance falls below a specified threshold, it is deemed that a conductive path (breakdown) has been established.

The local conductivity is proportional to the probability of the electron jumping between the neighbor centers, which exponentially depends on the distance between the centers:

$$\sigma_{ij} \sim \Gamma_{ij} = \gamma_{ij}^{0} exp\left(-\frac{2r_{ij}}{a} - \frac{\varepsilon_{ij}}{k_B T}\right)$$

The local resistor between i and j centers:

$$R_{ij} = R_{ij}^{0} exp\left(\frac{2r_{ij}}{a} + \frac{\varepsilon_{ij}}{k_B T}\right)$$

The primary focus is on the impact of r_{ij}, with the remaining parameters treated as constants.

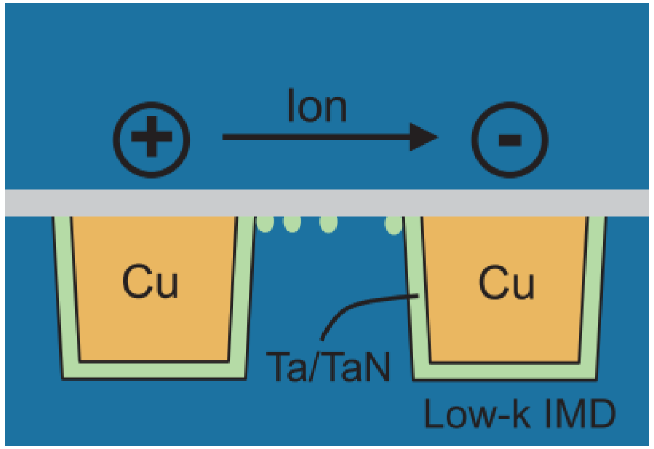

r_{ij} : The distance between i and j centers

a : The radius of electron localization at this type of centers

ε_{ij} : The energy barrier between i and j centers

The EPG-Based TDDB Model

Local Resistance and Ion Concentration

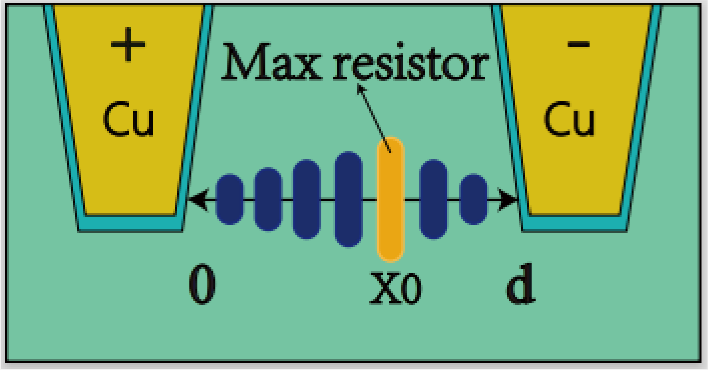

(a) Resistors distribution in IMD along path (0, d)

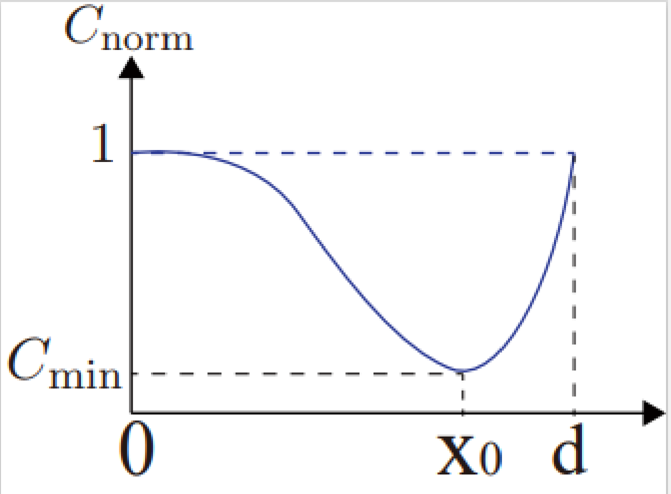

(b) Distribution of ion concentration

In a 2D system, the distance r_{ij} is determined by:

$$\boxed{r_{ij} = N(x, y, t)^{-1/2}}$$

$$R_{ij} = R_{ij}^{0} exp\left(\frac{2r_{ij}}{a} + \frac{\varepsilon_{ij}}{k_B T}\right)$$

Breakdown is considered to occur when the maximum local resistance is below a threshold, hence it is necessary to obtain the distribution of ion concentration at various positions over time.

Derivation of Ion Concentration Distribution

- **Define normalized ion concentration:**

$$C_{norm}(x, y, t) = C(x, y, t)/C_0$$

- **The diffusion of ions in an electric field:**

$$\frac{\partial C_{norm}}{\partial t} = -\nabla J$$

$$J = -D\nabla C_{norm} + v_d C_{norm}$$

$$where\ D = D_0 exp\left(-\frac{E_a}{k_B T}\right), v_d = \frac{qDE}{k_B T}$$

- **With boundary conditions:**

$$C_{norm}(x = 0) = C_{norm}(x = d) = 1$$

Solving the equations yields the ion concentration distribution, thus determining the TTF. However, utilizing these equations for TDDB analysis across the entire chip demands substantial hardware computing resources.

simplify the model

Model Simplification

□ Pre-simulation of 552 different patterns

TTF(s)	Count	Percentage
360000	42	7.61%
370000	269	48.73%
380000	194	35.14%
390000	34	6.16%
400000	11	1.99%
410000	2	0.04%

Statistics of TTFs in different patterns with the same minimum distance (50 nm)

TTF(s)	Count	Percentage
58000	23	4.17%
59000	159	28.80%
60000	219	39.67%
61000	78	14.13%
62000	30	5.43%
63000	12	2.17%
64000	18	3.26%
65000	13	2.36%

Statistics of TTFs in different patterns with the same minimum distance (20 nm)

□ The following conclusions are observed:

- The distribution of Time-To-Failure (TTF) is relatively concentrated, and the pattern of interconnections has a minimal impact on TTF.
- The minimum spacing between metal lines has a significant influence on TTF.
- As the spacing between metal lines decreases, its impact on TTF becomes more pronounced.

Model Simplification

- **The original TDDB model is simplified to the 1-D diffusion of ions between two parallel metal lines with the minimum spacing.**

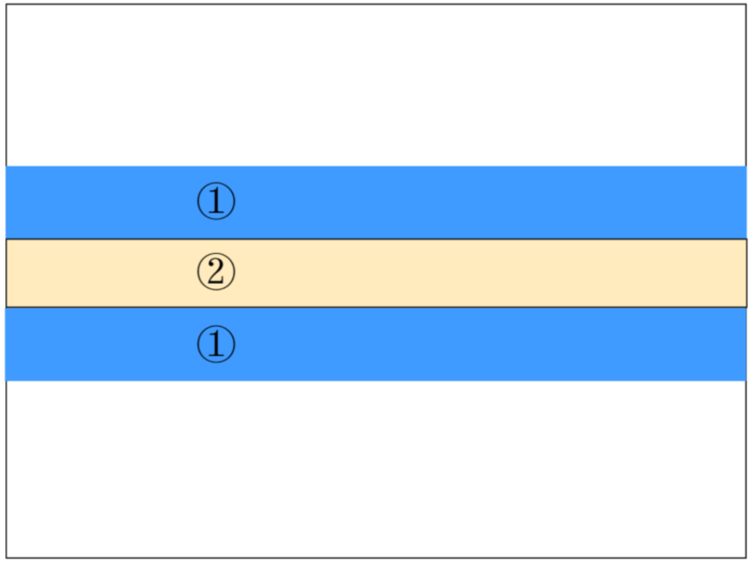

Schematic diagram of the simplified EPG-based TDDB model

The original equation can be rewritten as:

$$D\frac{\partial^2 C}{\partial x^2} = \frac{qDE}{k_B T}\cdot\frac{\partial C}{\partial x} + \frac{\partial C}{\partial t}$$

The boundary condition:

$$C(x=0) = C(x=L) = 1$$

The initial condition:

$$C(x,t) = 0, \qquad 0 < x < L, t = 0$$

The simplification to a 1-D model significantly reduces computational complexity, but its validity requires verification.

Model Validation

- Several common patterns are solved using the TDDB models before and after simplification separately.

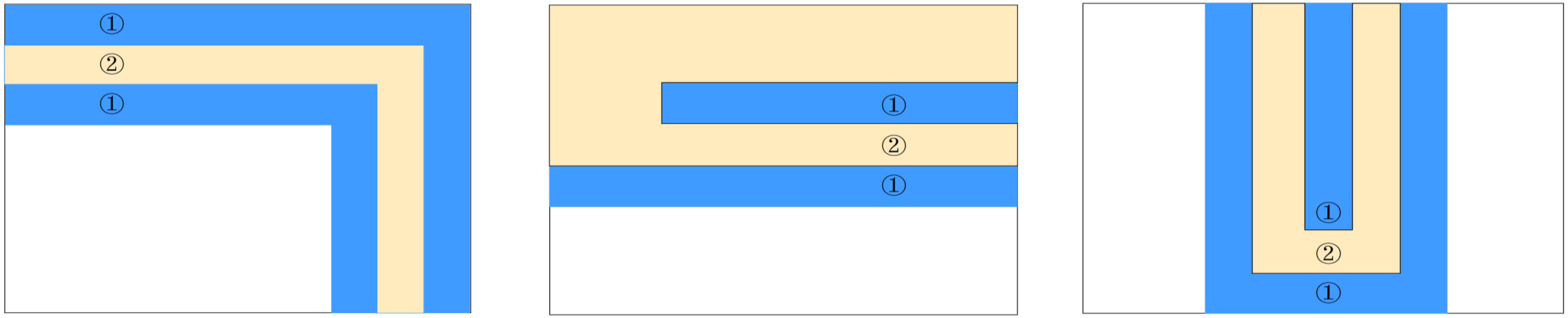

Three common metal line patterns

- COMSOL is employed to simulate the above three patterns.

Paras	Value	Paras	Value
D_0	$2.24 \times 10^{-11} \mathrm{m}^2/\mathrm{s}$	E_a	0.8eV
ε_{perm}	2.9	k_B	$1.38 \times 10^{-23} \mathrm{J/K}$
T	370K	V_{DD}	1V

The parameters used in the analysis

Model Validation

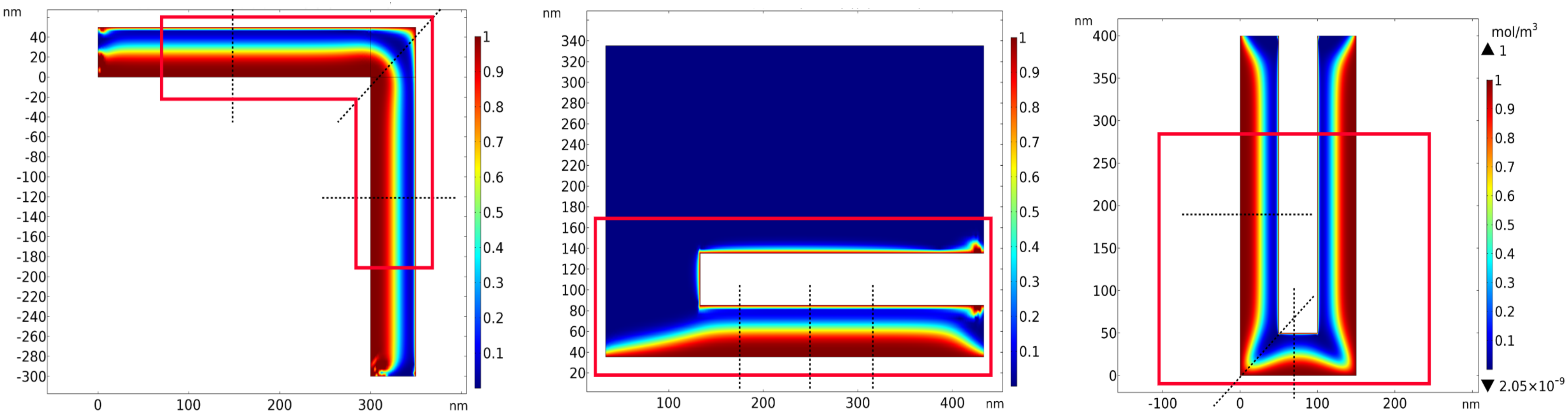

Simulation results of three patterns (focus on the ion concentration distribution along specific paths)

□ Comparing with infinite parallel metal lines, the following observations are made:

- The ion diffusion speed at the parallel sections in all three patterns is consistently greater than at the bent sections.
- The ion diffusion trends at the parallel sections in the three patterns closely resemble those of the infinite parallel metal lines.

Based on the observations and the principle of conservative analysis, the simplified 1-D model with two parallel metal lines is a reasonable substitution for the origin one.

Employment of PINN

Solution objective: $$D\frac{\partial^2 C}{\partial x^2} = \frac{qDE}{k_B T}\cdot\frac{\partial C}{\partial x} + \frac{\partial C}{\partial t}$$

Boundary conditions: $$C(x=0) = C(x=L) = 1$$ $$C(x,t) = 0, \qquad 0 < x < L, t = 0$$

◻ PDE Modification

Differences in the scale of independent variables can present challenges when solving with PINN.

$$\boxed{m^2 D\frac{\partial^2 C}{\partial X^2} = m\cdot\frac{qDE}{k_B T}\cdot\frac{\partial C}{\partial X} + \frac{1}{n}\frac{\partial C}{\partial T}}$$

$$C(X=0) = C(X=L) = 1$$
$$C(X,T) = 0, \qquad 0 < X < L, T = 0$$

◻ Constructing PINN

input layer: $\mathcal{N}^0(x) = x \in \mathbb{R}^{d_{in}}$

hidden layer: $\mathcal{N}^\ell(x) = \sigma\left(\mathcal{W}^\ell\mathcal{N}^{\ell-1}(x) + b^\ell\right) \in \mathbb{R}^{N_\ell}$

output layer: $\mathcal{N}^L(x) = \mathcal{W}^L\mathcal{N}^{L-1}(x) + b^L \in \mathbb{R}^{d_{out}}$

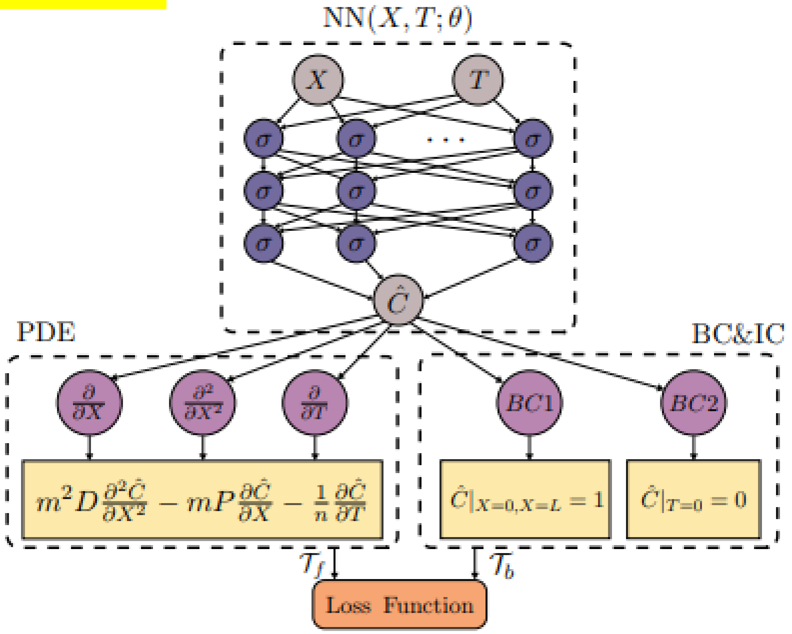

Schematic of the proposed PINN algorithm

Employment of PINN

☐ Loss Function

Embedding the physical PDE into the loss function of PINN.

Overall loss function:

$$\mathcal{L}(\theta;\mathcal{T}) = \omega_f \mathcal{L}_f(\theta;\mathcal{T}_f) + \omega_b \mathcal{L}_b(\theta;\mathcal{T}_b)$$

Within the interior of the solution domain:

$$\mathcal{L}_f(\theta;\mathcal{T}_f) = \frac{1}{|\mathcal{T}_f|}\sum_{x\in\mathcal{T}_f}\left\| m^2 D \frac{\partial^2 \hat{C}}{\partial X^2} - m \cdot \frac{qDE}{k_B T} \cdot \frac{\partial \hat{C}}{\partial X} - \frac{1}{n}\frac{\partial \hat{C}}{\partial T}\right\|_2^2$$

At the boundary of the solution domain:

$$\mathcal{L}_b(\theta;\mathcal{T}_b) = \frac{1}{|\mathcal{T}_b|}\sum_{x\in\mathcal{T}_b}\left\|\mathcal{B}(\hat{C},x)\right\|_2^2$$

☐ Configuration of PINN

Parameters	Value
Number of hidden layers	3
Number of neurons per layer	20
Activation function	Tanh
Optimizer	Adam
Training set size	$|\mathcal{T}_b| = 796 \ \ |\mathcal{T}_f| = 39204$
Number of iterations	20000
Loss weights	$\omega_f = 1\times10^{-7}, \omega_{bc} = 0.005, \omega_{bi} = 0.005$
Learning rate	5×10^{-4}

3. Results and Discussions

Solution of the Diffusion Equation

□ Solving the PDEs using FEM and PINN separately

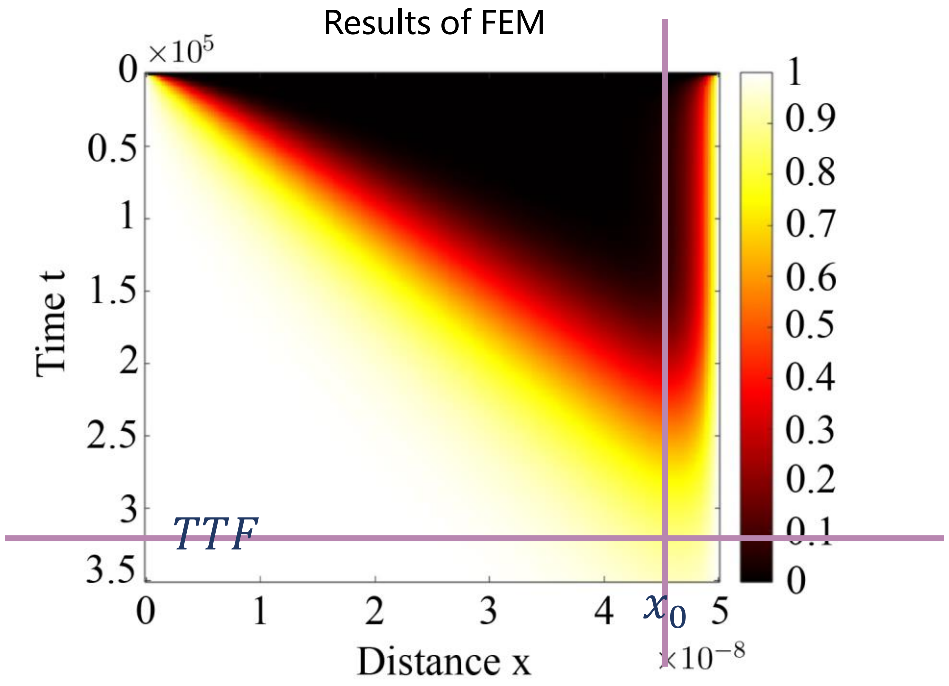

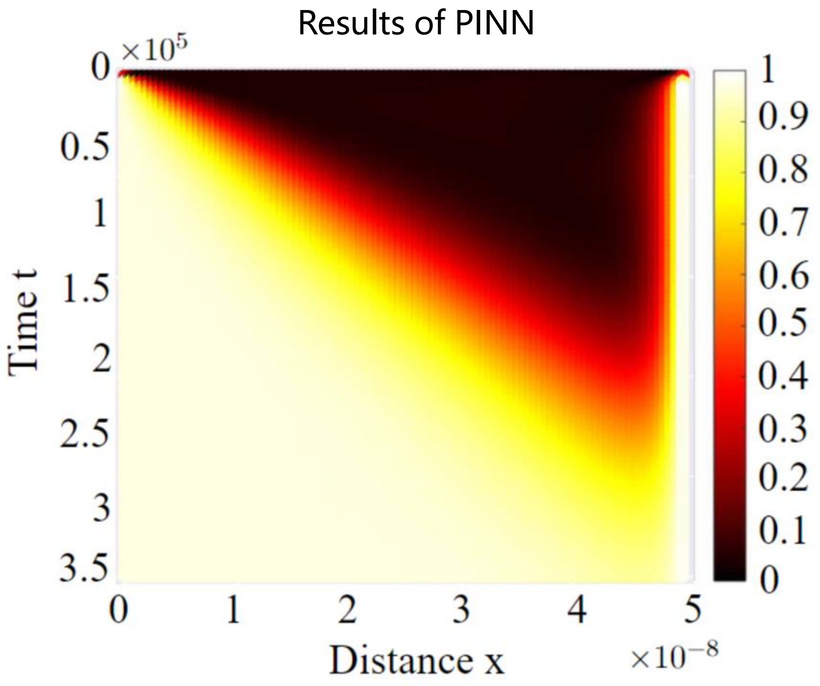

□ PINN and FEM results exhibit similar trends

- The ion concentration steadily increases over time.
- At any given moment, the minimum ion concentration (maximum local resistance) is located at x_0.

Accuracy Analysis

☐ The boundary conditions are discontinuous:

$$C(X=0)=C(X=L)=1$$

$$C(X,T)=0, \qquad 0<X<L, T=0$$

Neural network is always a composite of continuous functions.

☐ The contributions of different loss terms to the gradient are unbalanced:

$$\mathcal{L}(\theta;\mathcal{T})=\omega_f\mathcal{L}_f(\theta;\mathcal{T}_f)+\omega_b\mathcal{L}_b(\theta;\mathcal{T}_b)$$

Significant absolute errors are observed at the initial and upper-boundary points.

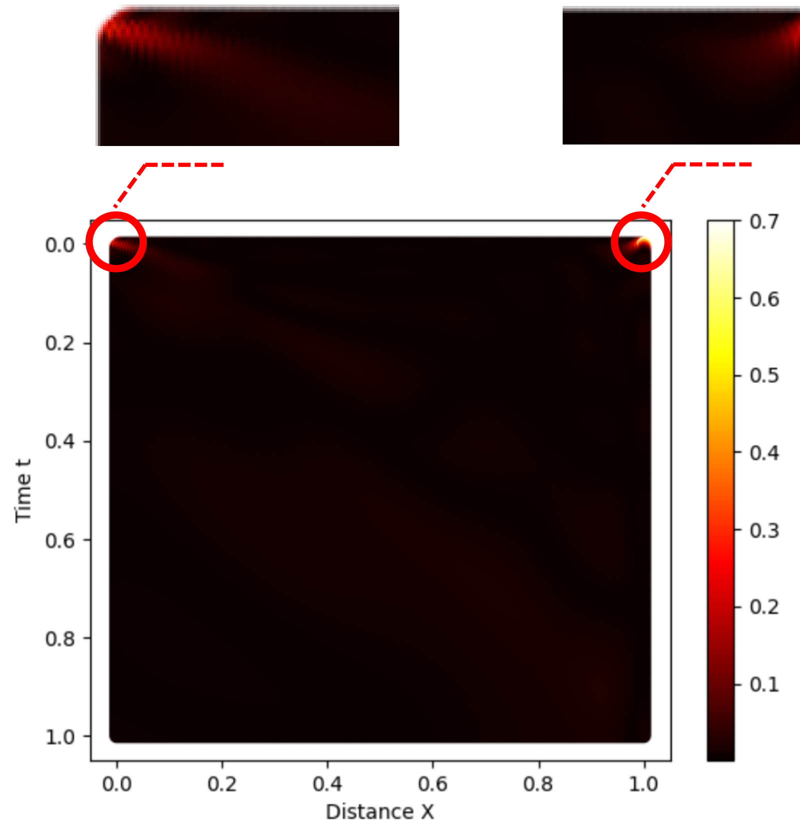

The absolute errors between PINN and FEM

Optimization Strategy

Making the boundary conditions continuous

Use exponential function to approach the boundary conditions.
The modified boundary condition is shown as follows:

$$C(0 \leq X < 0.1) = e^{-149.5X}$$

$$C(0.1 \leq X < 0.9) = 0, T = 0$$

$$C(0.9 \leq X \leq 1) = e^{-149.5(1-X)}$$

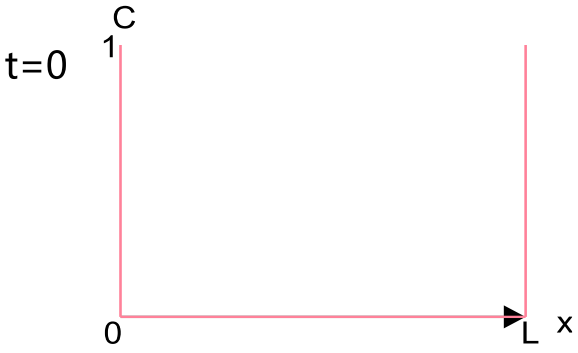

Original boundary conditions

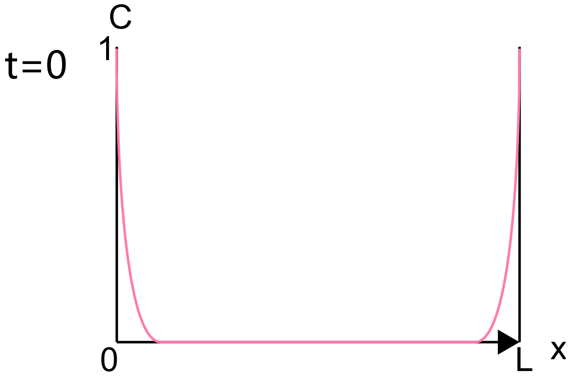

boundary conditions after continuous approximation

Applying hard constrain

Transform the output layer of PINN to ensure that the output values satisfy fixed boundary conditions.
The following transformation is applied to the output layer:

$$\boxed{C_{new} = X(X-1)C + 1}$$

Comparison of Computation Speed

☐ Comparing the prediction time by PINN and the computation time by FEM

Mesh Density	PINN (s)	FEM (s)	MSE	Acceleration Ratio
200^2	0.0012	0.1641	10.35×10^{-5}	136.75
400^2	0.0042	0.3403	9.275×10^{-5}	81.02
600^2	0.0088	0.5358	8.806×10^{-5}	60.89
800^2	0.0162	0.7608	8.549×10^{-5}	46.96
1000^2	0.0231	0.9443	8.390×10^{-5}	40.87

- PINN prediction speed is significantly faster than the computation speed of FEM.
- Mean square error decreases with the increase in mesh density.

4. Summary and Prospects

Summary and Prospects

- In this research, we present a physics informed learning method for EPG-based TDDB assessment.
- The simplified EPG-based TDDB model can effectively retain the details of the original model and benefits from fast computation.
- The diffusion equation of ions in an electric field extracted from EPG-based TDDB model is solved by the proposed physics informed neural network.
- The continuous definite condition and hard constrain optimization methods are used for improving the performance of PINN in terms of accuracy and speed.
- PINN exhibits high accuracy with a competitive advantage in prediction speed, leading to about 100 times speedup with less than 0.1% mean squared error, which indicates the great potential for EPG-based TDDB assessment on full-chip.

Thank You!